Journal of Hydroinformatics

Journal of Hydroinformatics Vol 26 No 10, 2601 doi: 10.2166/hydro.2024.127

Theoretical investigation of hysteresis loops in free-surface flow under sluice gates for power-law channels

Bilal Belharti[a], Lyes Amara[b,*] and Ali Berreksi[a]

[a] Université de Bejaia, Faculté de Technologie, Laboratoire de Recherche en Hydraulique Appliquée et Environnement (LRHAE), 06000 Bejaia, Algérie
[b] Department of Civil Engineering and Hydraulics, Faculty of Technology, LGCE Laboratory, University of Jijel, Ouled Aissa, Jijel 18000, Algeria
*Corresponding author. E-mail: lyes.amara@univ-jijel.dz

ABSTRACT

In the present study, a new theoretical framework and analytical solutions to the problem of hysteresis loops due to hydraulic jump in power-law open channels under supercritical flows are introduced. This investigation primarily focuses on the flow dynamics encountered at a vertical sluice gate across channels of various shapes: rectangular, parabolic, and triangular. By the application of energy and momentum conservation principles, the dual flow configurations emerging under identical initial conditions are shown. An intensive analytical computational analysis led to the development of approximate theoretical models, facilitating the prediction of hysteresis loops for a wide range of Froude numbers and dimensionless channel geometry parameters. Several illustrative examples were treated and the results show a high degree of accuracy of the proposed models in predicting the hysteresis loops. The present research contributes to a novel methodology for enhancing predictions regarding the behavior of supercritical flows and the design of open channels for specific scenarios of the hysteresis phenomenon.

Key words: analytical solution, contraction coefficient, hydraulic jump, hysteresis loops, power-law channels, sluice gate, supercritical flow

HIGHLIGHTS

- An analytical approach for the prediction of hysteresis loops in power-law channels is proposed.
- Explicit simplified models for facilitating the hysteresis loops prediction are given.
- An original approximate solution for the contraction coefficient induced by sluice gates is proposed.
- Results show a very satisfactory agreement between the models derived from the suggested approach and the few results found in the literature.

NOTATION

A	the wetted cross-sectional area of the channel (m^2)
a	gate opening (m)
a_{max}	maximum gate opening (m)
a_{min}	minimum gate close (m)
B	top width of rectangular channel (m)
C	correlation model constant
C_c	contraction coefficient
D	hydraulic diameter (m)
E	specific energy (m)
F_{r0}, F_{r1}, F_{r2}	Froude number of incident flow, flow immediately upstream of the gate, and flow downstream of the gate, respectively
g	acceleration due to gravity (ms^{-2})
K	correlation model constant
κ	shape factor of the parabolic channel
$\overline{\kappa}$	dimensionless parameter of the parabolic channel
m	shape factor of the triangular channel
$\overline{m}$	dimensionless parameter of the triangular channel
n	Manning's roughness coefficient

P	matching coefficient
Q	flow rate ($m^3\ s^{-1}$)
$\overline{Q}$	flow per unit of width ($m^3\ s^{-1}\ m^{-1}$)
q	specific discharge of the rectangular channel ($m^3\ s^{-1}\ m^{-1}$)
R	correlation coefficient
S	channel bottom slope
T	top width of parabolic and triangular channels (m)
u	flow velocity ($m\ s^{-1}$)
y_0	incoming flow depth (m)
y_1	flow depth immediately upstream of the gate (m)
y_2	flow depth downstream of the gate (zone of maximum contraction) (m)
α, β	factor shape of a power-law channel
χ	alternate depth ratio
η	aspect ratio
λ	hysteresis loop extent (m)
θ	the angle of inclination of the sidewalls to the horizontal of the triangular channel (°)
ω	conjugate depth ratio
ψ	the filling rate upstream of the gate

1. INTRODUCTION

In supercritical free-surface flows, the introduction of an obstacle into a channel or the modification of a geometric configuration such as a contraction, bed hump, or sluice gate often induces disturbance in the main flow. It results in a transition from supercritical to subcritical states, a process widely recognized as a hydraulic jump. This phenomenon exhibits a particular behavior; the possibility of two distinct flow configurations arising under identical initial conditions. This non-uniqueness in flow solutions is influenced not only by the geometric characteristics of the obstacle and the incoming flow but also by the dynamic evolution of the flow conditions themselves (Mehrotra 1975; Pratt 1983; Lawrence 1987; Defina & Susin 2003, 2006; Viero & Defina 2017, 2019). This behavior is indicative of the hysteresis effect associated with flows encountering obstacles, known as hydraulic jump hysteresis and the dual curve of the hydraulic system response during a cycle is defined as the hysteresis loop.

The theoretical foundations and experimental validations of hysteresis behavior have been thoroughly documented. Early works on this phenomenon, during the transition from supercritical to subcritical flow, were made by Abecasis & Quintela (1961, 1964) and Quintela & Abecasis (1979), with further empirical and theoretical expansions by Muskatirovic & Batinic (1977), Pratt (1983), Baines (1984), Austria (1987), and Lawrence (1987). These studies collectively affirm that any form of obstruction within a supercritical flow inherently induces hydraulic hysteresis, and straightforward methodologies for its calculation have been proposed.

Using catastrophe theory, Austria (1987) developed a descriptive model to elucidate the hysteresis observed in flows over a sill. The fundamental energy and momentum equations were used together with experimental validations to reinforce the model predictions. Conversely, Lawrence (1987) adopted an experimental approach for classifying flow regimes around a fixed obstruction, building upon Baines' (1984) earlier work involving a moving barrier. These experimental inquiries have been pivotal in demonstrating the existence of hysteresis loops, where two flow states coexist under identical conditions, thereby revealing the extent of hysteresis.

In a combined theoretical and experimental endeavor, Defina & Susin (2003) examined the flow through a vertical sluice gate within a rectangular channel, and showed that hysteresis loops can occur in both supercritical and subcritical flows, contingent on the Froude number exceeding 0.8. Their subsequent exploration of various obstacles within a rectangular channel further delineated the theoretical boundaries of the hysteresis region, affirming that flow states can be accurately predicted through the Froude number and the geometric attributes of the obstacle, with experimental outcomes aligning with theoretical forecasts, especially when the obstruction does not alter the channel's geometry.

A comprehensive study by Defina & Viero (2010) explored the dynamics of flow through a linear channel contraction, both theoretically and experimentally. Their work introduced a quasi-2D model for predicting shock wave patterns through such contractions. Notably, discrepancies were observed between the theoretical predictions and experimental outcomes, particularly concerning the transition paths between stable flow states. This discrepancy highlighted the existence of two distinct types of hysteresis loops: minor and major, each characterized in detail.

Achour & khattaoui (2013) presented a theoretical investigation of hydraulic jump hysteresis due to the presence of a sill in a rectangular channel. Two configurations of incoming flow were analyzed; one generated by a bottom gate and the other by a steeply sloping spillway. The study aimed to present a theoretical approach for determining the threshold Froude number necessary for the emergence and the disappearance of the hydraulic jump, thereby enhancing the understanding of the hysteresis phenomenon in the design of energy dissipators.

Further investigations carried out by Viero & Defina (2017) on supercritical flow behaviors around obstacles revealed intricate flow patterns, both downstream and upstream, emphasizing the complexity of flow transitions through different obstacle types, such as positive steps and channel contractions.

Subsequent work by the same authors Viero & Defina (2019) focused on the nuances of flow through sluice gates, demonstrating the dual possibility of free and submerged flow states under identical inflow and gate opening conditions. This finding underlined the significance of the hysteresis effect in hydraulic systems, which was further validated by various experimental conditions.

Recent experimental investigations by Dhar *et al.* (2021) have shed light on the hysteresis effect associated with hydraulic jumps in closed and inclined rectangular conduits. This study demonstrated the effectiveness of applying continuity and momentum equations, along with considerations of turbulent viscosity, to achieve a more nuanced theoretical analysis of the phenomenon. Remarkably, the theoretical predictions were found to align closely with the experimental observations, underscoring the robustness of the analytical framework employed.

Recently, Daneshfaraz *et al.* (2022) analyzed the hysteresis effects on flows through channels subjected to sudden and gradual contractions. The study focused on the impact of hysteresis on the relative residual energy, flow depth, and longitudinal profile under different varying contraction scenarios. Their findings revealed a pronounced hysteresis behavior, markedly influencing the relative residual energy with an average increase exceeding 50%. Moreover, in scenarios involving a submerged hydraulic jump, the absence of hysteresis was consistently observed across all the experimental setups. A direct correlation was established between the expansion of the hysteresis region and the width of both sudden and gradual contractions, highlighting the relationship between channel geometry and flow dynamics.

Despite the considerable attention devoted to studying hysteresis phenomena through obstacles in channels with rectangular cross-sections, a gap remains concerning other channel profiles. To fill this gap, the present study consists of a theoretical analysis of the hysteresis loops for supercritical flow controlled by a vertical sluice gate within power-law channels, specifically targeting rectangular, parabolic, and triangular channel shapes as illustrated in Figure 1. These profiles are prevalently adopted in engineering applications, ranging from irrigation and water supply to hydropower projects, owing to their functional advantages. Additionally, the use of gates for flow control and upstream water level management underscores the practical significance of the present research contribution.

The primary objective of this work is to analyze the physical phenomenon of the hysteresis loops and derive explicit equations characterizing this complex flow behavior. Through a methodical parametric study enriched by extensive computational analysis of hysteresis loops, a simplified theoretical model for each channel profile is proposed. These models span a comprehensive range of Froude numbers and channel geometries, facilitating a nuanced understanding of the sensitivity of hydraulic systems to dimensionless parameters. This approach aims to deduce the extent of hysteresis loops for each channel profile, offering valuable insights for practitioners. Specifically, the methodology focuses on determining the maximum gate opening values that ensure the re-establishment of undisturbed flow conditions across the predefined channel geometries, essentially identifying the threshold gate opening required to eliminate the hydraulic jump from the channel. Furthermore,

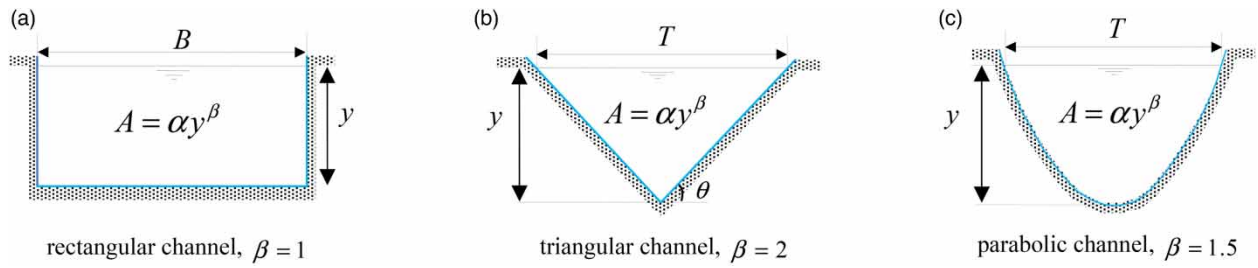

Figure 1 | Investigated channel shapes.

the comparative analysis of hysteresis loops across different channel profiles aims to enhance the understanding of hysteresis behaviors due to changes in flow parameters, thereby contributing to the enhancement of the design process in open channel engineering.

2. PHYSICAL DESCRIPTION OF THE PHENOMENON

The interaction between a vertical sluice gate and a supercritical flow in open channels hinges on the gate opening rate and the Froude number of the approaching undisturbed flow. This interaction delineates two distinct configurations of free-surface flow: (i) continuous undisturbed supercritical flow throughout the channel without interacting with the gate, when the gate opening is greater than the incident flow depth (Figure 2(a)) and (ii) the second case is when the gate opening is decreased until it touches the free surface of the incoming undisturbed flow. In this case, the water level upstream of the gate is increased, and a subcritical flow is established with the formation of a hydraulic jump, as shown in Figure 2(b). As the gate opening narrows, the water level upstream increases, propelling the hydraulic jump upstream against the flow direction until momentum equilibrium is reached. Conversely, gradual gate opening decreases the hydraulic jump sequent depth and drawing it closer to the gate, as shown in Figure 2(c). This gate position marks the threshold for establishing subcritical flow upstream. In addition, it is the same gate opening from which a supercritical flow passes under the gate without interacting with it. Beyond this point, further opening eliminates the hydraulic jump, and the original flow condition is restored. Thus, a unique gate opening can sustain two free-surface configurations, embodying the essence of hydraulic jump hysteresis where the current flow state is a function of its historical flow conditions (James 2020). Thus, the hysteresis is a phenomenon reflecting the fact that the history of the disturbance introduced in a supercritical regime (with the presence of a hydraulic jump) leads to a different path in the response of the system when the disturbance is removed. The 'memory' of the system is then involved and the hysteresis loops, defined by the response path curve during a gate operation cycle, must be determined exactly for a correct simulation of that system.

As a result of applying the theoretical analysis presented in the following sections, the hysteresis loop due to the hydraulic jump is illustrated in Figure 3, which represents an example of the variation of the water depth upstream of the gate as a function of the gate opening. The minimum value of gate opening at which undisturbed supercritical flow can be established along the channel without interaction with the gate is $a_{\min} = y_0$. The limiting value $a = a_{\max}$ represents the gate opening value so that undisturbed supercritical flow conditions are restored. The opening rates $a_{\min} < a < a_{\max}$ represent the values of a for a

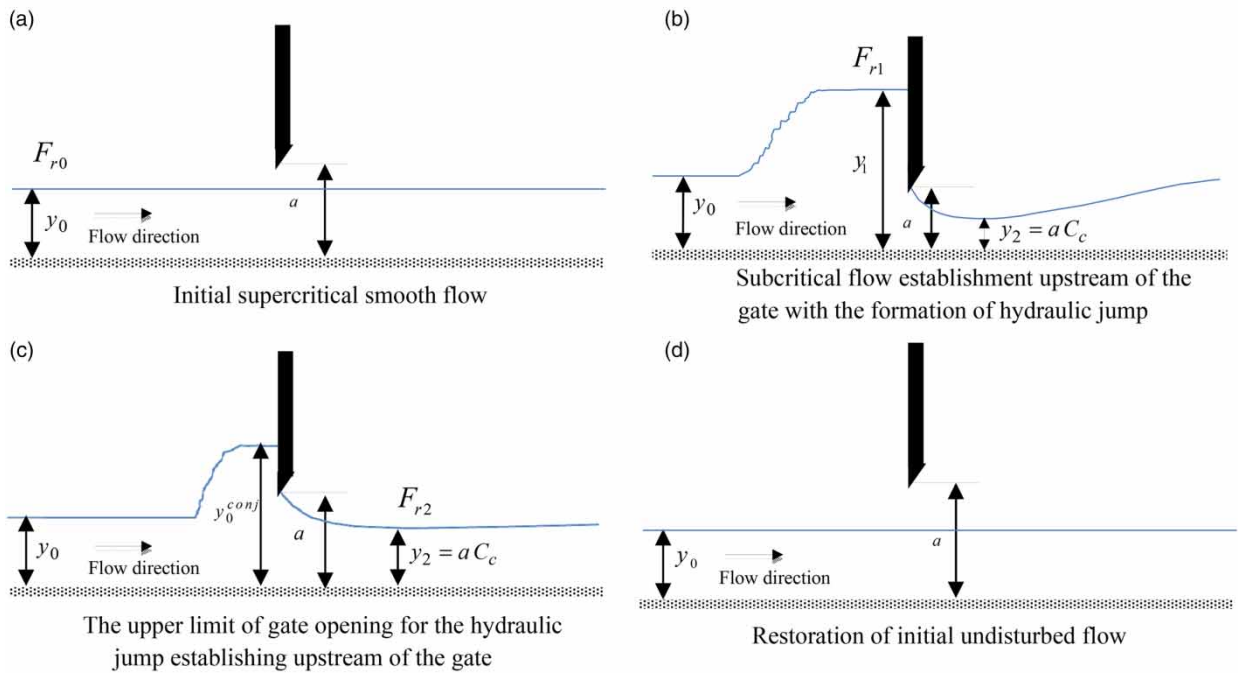

Figure 2 | The hysteretic behavior of a flow through a vertical sluice gate.

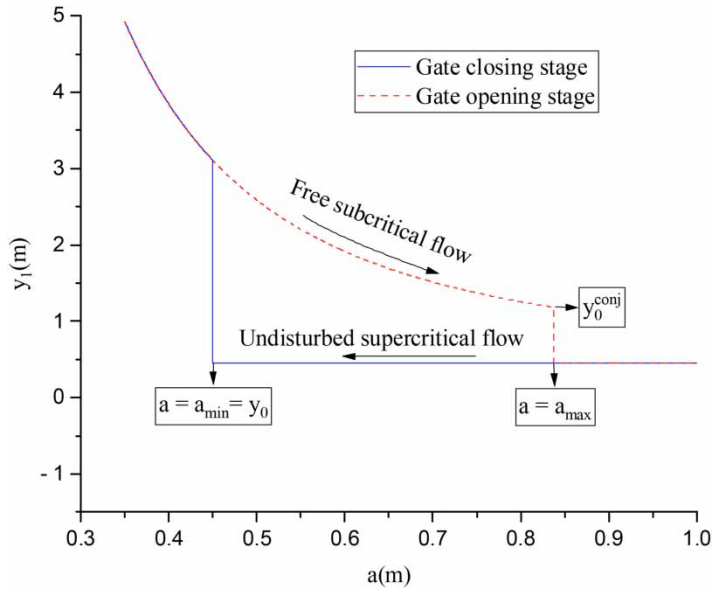

Figure 3 | Hysteretic cycle of a flow through a sluice gate.

subcritical flow established just upstream of the sluice gate with the formation of hydraulic jump. The hysteretic flow nature is well illustrated in Figure 3 by the fact that, for the same initial conditions, the flow outward and return paths are different. On the other hand, Figure 4 shows how the hysteresis phenomenon reacts to changes in the flow cross-section. In this case, a flow with the same momentum and incident Froude number was initiated in each of the three profiles. The obtained results indicate that the hysteresis behavior of the flow is significantly influenced by the cross-sectional area of the flow. Moreover, it was also found that the hysteresis loop extent for the same flow conditions is strongly related to the parameter $\overline{Q} = Q/T$, where Q and T are the discharge and the top width of the channel flow, respectively. The hysteresis loop extent then increases as the parameter $\overline{Q}$ increases.

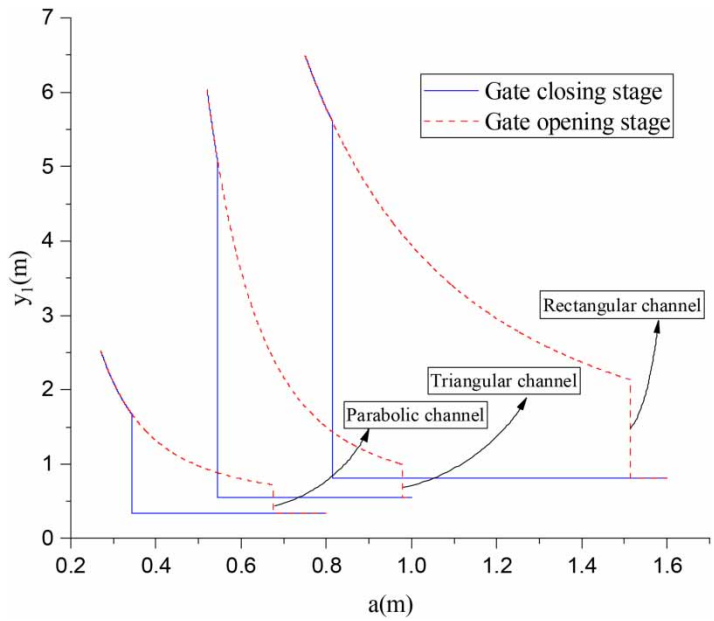

Figure 4 | Flow cross-section effect on hysteresis extent.

3. ENERGY AND MOMENTUM CONSIDERATIONS

3.1. Alternate depth ratio in power-law channels

In open channel hydraulics, the concept of alternate depths refers to two specific water depths that a given discharge can achieve under the same specific energy but in different flow regimes. This section presents the calculation of alternate depth ratios within power-law channels.

For a power-law-shaped channel profile, the cross-sectional area A and the water depth y are related together as follows:

$$A = \alpha y^{\beta} \tag{1}$$

where the parameters α and β determine the shape function of the cross-sectional profile. In the present study, three cross-sectional shape profiles are investigated, $\beta = 1$, $\beta = 1.5$, and $\beta = 2$, which correspond to rectangular, parabolic, and triangular channel shapes, respectively. These channel cross-sections are frequently used in practice.

It is well known that the flow Froude number is expressed as:

$$F_r = \frac{u}{\sqrt{gD}} \tag{2}$$

Therefore, from Equation (2) the velocity can be written as:

$$u^2 = F_r^2\, g\, D \tag{3}$$

where u is the flow velocity, $D = A/T$ is the hydraulic diameter, g is the acceleration due to gravity, and T is the top width. Using the expression of the top width $T = (dA/dy) = \alpha\beta y^{\beta-1}$, the hydraulic diameter is then expressed as $D = y/\beta$. When replaced in Equation (2), the kinetic parameter F_r^2 is given as follows:

$$F_r^2 = \frac{\beta Q^2}{g A^2 y} \tag{4}$$

The specific energy, on the other hand, is given by the expression (Chow 1959):

$$E = y + \frac{u^2}{2g} \tag{5}$$

According to the alternate depths definition, the specific energy is the same, such as $E_1 = E_2$.

Reporting the expressions of Equations (2) and (3) into Equation (5) gives, after simplification and rearrangement, the following:

$$\frac{y_1}{\beta}\left(\beta + \frac{1}{2}F_{r1}^2\right) = \frac{y_2}{\beta}\left(\beta + \frac{1}{2}F_{r2}^2\right) \tag{6}$$

Denoting $\chi = y_2/y_1$ and remarking that $(F_{r1}^2/F_{r2}^2) = (y_2/y_1)^{2\beta+1}$, Equation (6) reduces to (Pandey *et al.* 2018):

$$(\chi^{2\beta+1} - \chi)\, F_{r2}^2 - 2\beta(\chi - 1) = 0 \tag{7}$$

For a known downstream Froude number and channel shape (factor β), Equation (7) can be used to calculate the exact alternate depth ratio in a power-law channel. To do so, and for the investigated channel shapes, Equation (7) leads to an algebraic polynomial of nth order, whose solutions can be obtained analytically (up to the fourth order in accordance with the Abel-Ruffini theorem) using classical methods (Pandey *et al.* 2018) or even numerically. Quadratic, cubic, and quartic equations are obtained for rectangular, parabolic, and triangular-shaped channels, respectively. Since we are dealing with flow depths, the retained values of the polynomial roots should be real, positive, and consistent with the flow regime type.

3.2. Conjugate depth ratio in power-law channels

For a given momentum, the concept of conjugate depths refers to two specific depths at which the same discharge occurs, synonymous with the phenomenon of hydraulic jumps.

By denoting the conjugate depth ratio as $\omega = y_0/y_1$, and applying the momentum equation (Chaudhry 2008), the following equation for the conjugate depth ratio in terms of the incident Froude number and the channel shape is then obtained (Vatankhah 2017):

$$\omega^{\beta+1} - 1 = \frac{\beta+1}{\beta} F_{r0}^2 (\omega^{2\beta+1} - \omega^{\beta+1}) \tag{8}$$

Equation (8) is nonlinear (i.e., non-unique in solutions), and its implicit character prevents a direct analytical solution of the conjugate depth. To unify the solutions and produce an explicit equation, Vatankhah (2017) used the asymptotic matching technique, which consists of finding two distinct solutions to the problem, each of which is valid within a certain interval of values of the dependent variable ω. These two solutions are then combined together by a matching coefficient P to form a global solution.

The explicit form of the conjugate depth ratio equation is written as follows (Vatankhah 2017):

$$\omega = \left[\left(\frac{\beta+1}{\beta} F_{r0}^2 \right)^{-P/\beta+1} + F_{r0}^{-2P/2\beta+1} \right]^{1/P} \tag{9}$$

The coefficient P is given on the other hand by Vatankhah (2017) as:

$$P = 4.12\,\beta^{1.65} + 14.2 \left(\frac{\beta+1}{\beta} F_{r0}^2 \right)^{-0.83} \tag{10}$$

The approximate solution formed by Equations (9) and (10) is used in the present analysis for the determination of the conjugate depths of the hydraulic jump.

4. FLOW CONTRACTION UNDER A SLUICE GATE

Gates are hydraulic structures commonly used for flow regulation, measurement in irrigation projects or on spillway crests, and for controlling upstream water levels. Flow through a vertical sluice gate can be free or submerged, depending on the tailwater depth.

Several analytical and experimental studies have investigated the flow behavior under gates; many of them have found that there are significant deviations between the mathematical models and the experimental measurements (Montes 1997).

One of the most determining factors influencing flow behavior beneath gates is the contraction coefficient C_c (Figure 2(b) and 2(c)). The task of estimating the contraction coefficient has attracted much experimental and theoretical research under free and submerged flow conditions. Despite the comprehensive research dedicated to the contraction coefficient, uncertainties in its calculation persist, attributed to the complex nature of flow behavior under the sluice gate. This complexity is compounded by variables such as turbulence and vortex formation. Among the seminal and most influential contributions, the classical hydrodynamic theories of Cisotti (1908) and Von Mises (1917) stand out. These theories apply potential flow theory through conformal mapping but do not account for gravitational effects (Montes 1997). Following in this theoretical lineage, Pajer (1937) and Marchi (1953) maintained the resolution's philosophical core by employing conformal mapping theory, yet they innovatively incorporated the approximate integration of gravitational effects, specifically the variation in flow velocity along the section downstream from the gate. Furthermore, the application of numerical methods by researchers such as Issacs (1977), Betts (1978), Montes (1997), and Vanden-Broeck (1997) underscores the multidimensional approach to understanding flow contraction. The results of experimental investigations conducted by Benjamin (1956), Rajaratnam & Subramanya (1967), Rajaratnam (1977), Rajaratnam & Humphries (1982), Roth & Hager (1999), Yen *et al.* (2001), and many others later are to be cited in this regard.

In the following section, the derivation of an explicit expression for the contraction coefficient obtained from the implicit Von Mises equation is developed. According to Von Mises (1917), the contraction coefficient C_c depends only on the parameter ψ which is the ratio between the sluice gate opening a and the water level upstream of the gate y_1, that is, $\psi = a/y_1$. The contraction coefficient C_c is written as follows (Von Mises 1917):

$$C_c^{-1} = 1 + \frac{2}{\pi}\left[\frac{1}{C_C\psi} - C_c\psi\right]\tan^{-1}(C_c\psi) \tag{11}$$

The core idea of the explicit approximation involves the expansion of the implicit Von Mises equation using a Taylor series, leading to a polynomial equation that can be solved analytically. It is evident that with increasing the order of the Taylor series expansion, the deviation between the implicit and explicit solutions diminishes. Nevertheless, the complexity of achieving an analytical solution increases, eventually becoming impracticable. Consequently, to maintain solvability, the Taylor series expansion is truncated to a certain order leading to a cubic equation, thus facilitating the use of trigonometric functions for the solution derivation.

It is important to note that Von Mises' theory was originally formulated for the contraction coefficient for plane problems, making it ideally applicable for wide rectangular channels. Since so far, no other theory exists for the confinement effect (wall effect), the same theory is considered to hold for triangular and parabolic-shaped channels.

The derived explicit analytical solution to the implicit Von Mises equation, which makes use of trigonometric functions, is obtained by first denoting $x = C_c$ and expanding Equation (11) in a Taylor series. One obtains:

$$\frac{1}{x} = 1 + \frac{2}{\pi} - \frac{8}{3}\frac{\psi^2 x^2}{\pi} + \frac{16}{15}\frac{x^4\psi^4}{\pi} - \frac{24\psi^6 x^6}{35\pi} + \mathrm{O}(x^8) \tag{12}$$

where $\mathrm{O}(x^8)$ is the higher order term, which means that by truncating this equation to that order, we must accept an error in the order of x^8.

To be able to solve Equation (12) analytically, one must truncate the Taylor series expansion to the third order, which can be solved using trigonometric functions. Thus Equation (12) reduces to:

$$x^3 - \left(\frac{3\pi + 6}{8\psi^2}\right)x + \frac{3\pi}{8\psi^2} = 0 \tag{13}$$

Equation (13) is a cubic equation that can be written in the form $x^3 + ax^2 + bx + c = 0$ where $a = 0$; $b = -(1/8)((3\pi + 6)/\psi^2)$; and $c = 3/8\ \pi/\psi^2$. Denoting $\Omega = (3b - a^2)/9$ and $\Pi = (9ab - 27c - 2a^3)/54$, then the values of the discriminant $\Delta = (\Omega^3 + \Pi^2) < 0$ and all roots are real and unequal. The retained solution satisfying the condition $0.611 \leq C_c \leq 1$ is then (Zwillinger 2018):

$$x_3 = 2\sqrt{-\Omega}\cos\left(\frac{1}{3}\theta + 240^\circ\right) - \frac{1}{3}a \tag{14}$$

where

$$\theta = \cos^{-1}\left(\frac{\Pi}{\sqrt{-\Omega^3}}\right) \tag{15}$$

After simplification, the final expression for the approximate solution of C_c reads then as follows:

$$C_c = \frac{\sqrt{2\pi + 4}\cos\left(\pi/3 + (1/3)\cos^{-1}\left(3\pi\sqrt{2}\psi/(\pi + 2)^{3/2}\right)\right)}{2\psi} \tag{16}$$

Figure 5 shows the solution for both the original implicit equation and the proposed approximate solution.

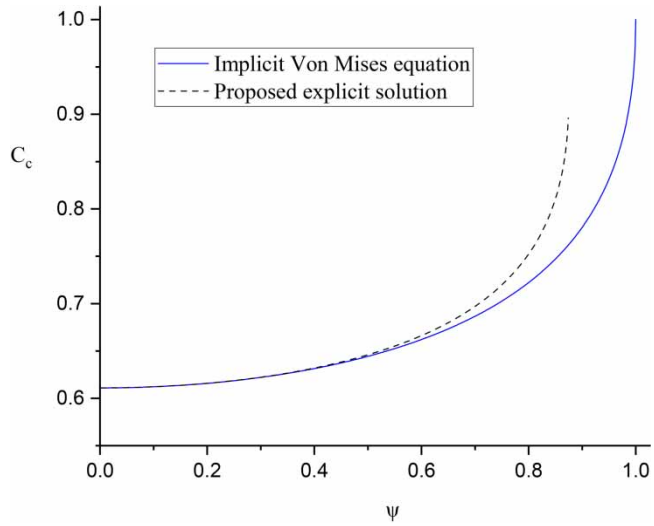

Figure 5 | Contraction coefficient as function of the ratio $\psi = a/y_1$ from the implicite Von Mises equation and the proposed explicit relationship (16).

Equation (11) reproduces the particular cases for which, when $\psi \to 0$, the contraction coefficient C_c takes the limit value of $\pi/(2+\pi) = 0.611$, and when $\psi \to 1$ the contraction coefficient takes the upper limit value of 1. However, the present approximate solution (Equation (16)) is valid for values of ψ up to 0.75. Beyond this value, the deviation between the two solutions tends to become significant. This is due to the singularity of the tangent function in the vicinity of $\theta = \pi/2$. This singularity introduces inaccuracies in the Taylor series approximation, as it trends toward an infinite vertical asymptote, a behavior unattainable by any finite Taylor series expansion. In the present case and throughout the study, the ratio $\psi = a/y_1$ is always in the range where the contraction coefficient solutions given by the two approaches are very close.

The approach detailed above is applicable for initial flow conditions that are purely supercritical ($F_{r0} \geq 1$). In this paper, we have focused on Froude numbers ($F_{r0} \geq 2$), to avoid errors in estimating the conjugate depth of the hydraulic jump (y_1), since when the Froude number of the incident flow is less than approximately 2, the hydraulic jump in this case is considered undular, and present secondary waves (Favre waves) and instability of the free-surface flow lead to increased errors as a result. For this reason, the analyses are carried out from a Froude number equal to 2 in the series of hysteresis loop computations so that the formulas obtained in the present study are free from the secondary effects induced by the Froude numbers between 1 and 2.

5. INTENSIVE COMPUTATION OF HYSTERESIS LOOPS

5.1. General procedure

To study the hysteresis phenomenon within power-law channel flows, intensive numerical computations were conducted with the ultimate goal of developing a simplified approximate model for engineering design purposes. This tool is envisioned to simplify the process of selecting the most suitable channel cross-section for engineering projects, by providing a direct means to evaluate the hysteresis effect without the need for repeated, detailed simulations for every conceivable variation in flow parameters or channel geometries. Such an endeavor traditionally requires significant computational effort and resources.

The methodology followed consists of an exhaustive computational analysis, meticulously carried out across a range of channel profiles and the deduction of approximate mathematical models.

For each channel profile, a detailed computational analysis was performed, starting with the definition of the channel geometry and flow parameters. The analysis began by adjusting the operation range of the sluice gate from an initial opening wider than the water depth of the incident flow ($a_{max} > y_0$), to a final position where the sluice gate intersects the flow ($a_{max} < y_0$). The hysteresis curve, which represents the relationship between the water depth upstream of the gate and the

gate operational range, was plotted upon completing the gate's closing and opening cycle $y_1 = f(a)$ (Figure 3). The hysteresis curve is obtained when the sluice gate has completed the closing and opening phases.

Next, once the hysteresis curve is obtained, the ratio $\psi = (a/y_1)$ is calculated and inserted into Equation (16) to calculate the new contraction coefficient. If this last one is equal to the initial C_c used in the calculations, then the obtained curve is the desired one. Otherwise, the initial C_c takes the value of the new C_c calculated by Equation (16), and so on until $C_c\_new = C_c\_init$ is obtained. The procedure is repeated until the final hysteresis curve is obtained.

Finally, for each final hysteresis curve obtained, the ratio between the hysteresis loop extent $\lambda = a_{max} - a_{min}$ and the discharge per unit of width $\overline{Q}$ is taken, and plotted in a new graph as a function of the incident Froude number $\lambda/\overline{Q} = f(F_{r0})$ where F_{r0} ranges from 2 to 12. The procedure is repeated for all channel profiles for a wide range of cross-sectional shape parameters, which are discussed in the following section.

5.2. Dimensionless parameters

For the sake of results generalization, a number of dimensionless parameters were introduced. The extent of the hysteresis loops was then computed for a wide range of dimensionless parameters to cover the entire practical range. The first normalized parameter refers to the aspect ratio η defined as:

$$\eta = \frac{y_0}{T} \tag{17}$$

where y_0 is the water depth of the incident flow and T is the top width, which is taken by default to be equal to unity for calculating aspect ratio η in the series of computation for all channel profiles ($T = 1$).

On the other hand, $m = 1/\tan(\theta)$ is the parameter that controls the inclination of the sidewalls to the horizontal of the triangular channel, and the dimensionless parameter is:

$$\overline{m} = \frac{1}{2\eta} \tag{18}$$

For the parabolic channel, defining κ as a shape parameter such as $y = \kappa x^2$ where $x = T/2$, the dimensionless parameter in this regard is the flow depth normalized by the square of the half top width as follows:

$$\overline{\kappa} = 4\eta \tag{19}$$

In the present study, a specific transformation of the channel form was employed, where instead of using the actual channel dimensions, a standardized channel with a width of unity and a water depth equal to y_0/T was used. Consequently, the new flow $\overline{Q}$ will be defined as:

$$\overline{Q} = \frac{Q}{T} \tag{20}$$

For a rectangular channel, Equation (20) defines the specific discharge $q = Q/B$. However, for nonrectangular profiles, it is important to point out that this concept bears no relation to unit flow; it is merely a theoretical concept introduced to facilitate calculations. It can be viewed as a pure normalization technique rather than a physical concept. Table 1 concisely presents the range of dimensionless parameters employed throughout this series of computations. The range of dimensionless parameters, as summarized in Table 1, encompasses the variability in channel shapes and flow conditions, ensuring comprehensive coverage in the present analysis.

Table 1 | Range of dimensionless parameters used in the hysteresis loops computation

	Rectangular channel	Triangular channel		Parabolic channel	
Dimensionless parameter	$\eta = y_0/B$	$\eta = y_0/T$	$\overline{m} = 1/2\eta$	$\eta = y_0/T$	$\overline{\kappa} = 4\eta$
Range	$0.05 \leq \eta \leq 7$	$0.05 \leq \eta \leq 2.83$	$0.176 \leq \overline{m} \leq 1$	$0.01 \leq \eta \leq 2$	$0.04 \leq \overline{\kappa} \leq 8$

5.3. Computation steps of the hysteresis loops

The computation of hysteresis loops in open channels with power-law profiles involves systematic steps summarized as follows:

1. Channel shapes ($\beta = 1$, $\beta = 1.5$, and $\beta = 2$) corresponding to rectangular, parabolic, and triangular channel shapes, respectively, are selected.
2. The channel geometry and flow parameters are fixed (y_0, T, Q, F_{r0}, κ, m). The index 0 refers to the incident flow parameters.
3. The maximum opening and closing of the sluice gate and its operating increment are defined.
4. Using Equation (17), the aspect ratio η is computed.
5. Compute the new flow per unit of width $\overline{Q}$ from Equation (20).
6. From Equations (18) and (19), the new cross-sectional shape parameters $\overline{m}$ and $\overline{\kappa}$ are computed for triangular and parabolic channel shapes, respectively.
7. From Equation (10), the coefficient P is calculated.
8. The P value is inserted into Equation (9) to calculate ω.
9. Calculate the conjugate water depth $y_0^{\text{conj}} = y_0/\omega$ upstream of the sluice gate.
10. For each gate opening step, calculate F_{r2} by using Equation (4).
11. By referring to Equation (16), calculate the contraction coefficient in such a way that one obtains C_c_new $= C_c$_init.
12. Following the channel shape, Equation (7) is used to compute the water depth immediately upstream of the sluice gate y_1.

The series of computations from step 10 will be repeated for each sluice gate opening and closing step. Because the approach discussed in this paper requires a large amount of calculation, a computational code written in Matlab was developed to ensure the complete calculation of the aforementioned algorithm for the hysteresis loops.

5.4. Sample computational results

After conducting intensive computations of the hysteresis loops based on the aforementioned procedure, an example of the bundle of curves obtained is shown in Figure 6. Each of the resulting curves represents an independent scenario characterized by its own combination of flow parameters and channel geometry. Remarkably, the results exhibit a self-similar pattern, suggesting that the approximate mathematical model should be described by a functional that combines exponential and power-law functions. The application of that combined model leads to results characterized by a coefficient of determination R^2 greater than 0.999, which is similar for all investigated channel shapes.

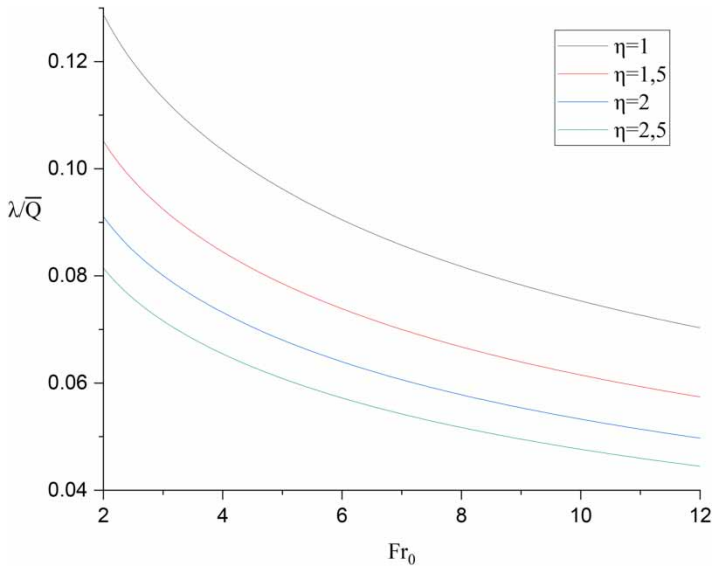

Figure 6 | Example of a bundle of curves obtained with different aspect ratios η.

6. PROPOSED DIRECT SOLUTION FOR HYSTERESIS LOOPS COMPUTATION

To obtain a unique general analytical expression for calculating the extent of hysteresis loops for different channel profiles, the curves in Figure 6 must collapse into a single curve to obtain a unique equation that relates the extent of hysteresis loops to the Froude number and the cross-sectional shape parameter for each channel profile. Formally, the self-similarity principle along with the dimensional analysis technique was used (Sedov 1959; Barenblatt 1996) and the procedure has led to the following functional relationships:

- $\frac{\lambda}{\overline{\overline{Q}}} = f(F_{r0},\ \eta)$ for the rectangular channel,
- $\frac{\lambda}{\overline{\overline{Q}}} = f(F_{r0},\ \overline{\kappa})$ for the parabolic channel,
- $\frac{\lambda}{\overline{\overline{Q}}} = f(F_{r0},\ \overline{m})$ for the triangular channel.

Through an in-depth correlation analysis of the obtained curves for each channel profile, approximate theoretical models for a direct hysteresis loop computation were obtained (Table 2). The proposed models showed exceptionally high correlation coefficients ($R^2 > 0.999$) with a very confined maximum deviation of approximately 1%, as shown in Figure 7 and summarized in Table 2. The present explicit models consequently form a very precise theoretical approach, especially for engineering purposes, without resorting to tedious nonlinear equation solutions, often requiring a lengthy process of trial and error.

Table 2 | Equations of proposed models for calculating hysteresis in power-law channels

Channel shape	Model equation	Parameters	Maximum relative error (%)
Rectangular channel	$\frac{\lambda}{\overline{\overline{Q}}} = \frac{1}{\sqrt{\eta}} C F_{r0}^{-K}$	$K = 0.337$ $C = 0.164$	1
Triangular channel	$\frac{\lambda}{\overline{\overline{Q}}} = \sqrt{\overline{m}}\, C F_{r0}^{-K}$	$K = 0.535$ $C = 0.71$	1.4
Parabolic channel	$\frac{\lambda}{\overline{\overline{Q}}} = \frac{1}{\sqrt{\overline{\kappa}}} C F_{r0}^{-K}$	$K = 0.443$ $C = 0.621$	0.71

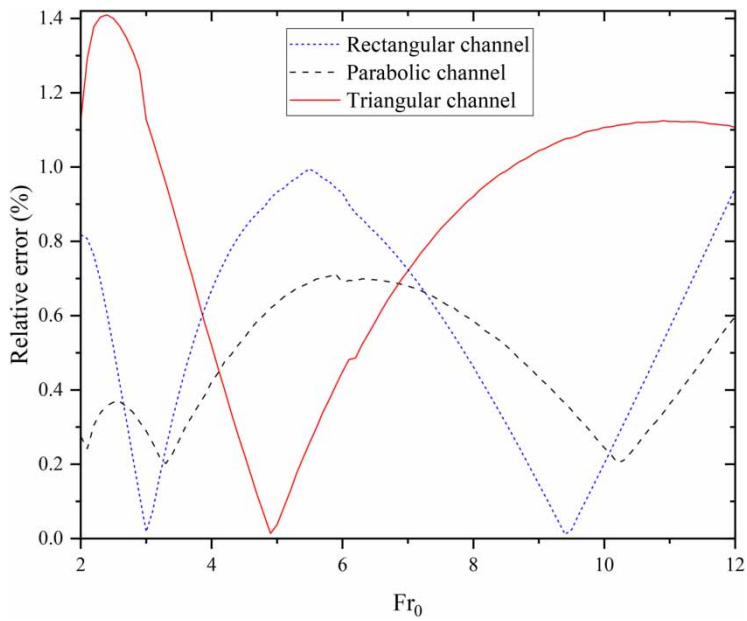

Figure 7 | Maximum relative error of the proposed approximate models as function of the incident Froude number.

7. PRACTICAL APPLICATIONS

7.1. Application 1

The first application example is taken from experimental data of Defina & Susin (2003). A flow of 1.25 $m^3 s^{-1}$ with a water depth of 0.65 m is conveyed in a rectangular channel of 0.38 m wide. The maximum gate opening required to restore the initial flow conditions is then to be determined. When the gate is moved down from 1.3 to 0.55 m, then it returns to 1.3 m. Note that the Froude number of the incident flow is $F_{r0} = 2$.

It follows that $\eta = y_0/1 = 0.65/1 = 0.65$. From Equation (20), $\overline{Q} = Q/B = 1.25/0.38 = 3.29\ m^3\ s^{-1}\ m^{-1}$. Using Equation (10), $P = 6.6477$, and from Equation (9) one obtains $\omega = 0.4203$, which leads to $y_0^{conj} = y_0/\omega = 0.65/0.4203 = 1.5465$ m. Using Equation (4), F_{r2} is calculated for each sluice gate step.

Replacing the value of $F_{r2} = 4.152$ when $(a = y_0)$ in Equation (7) gives the water depth immediately upstream of the gate $y_1 = 3.804$ m in order to obtain $C_c\_new = C_c\_init$. Repeating the process from step 10 for each gate opening one obtains $\lambda/\overline{Q} = 0.1597\ s\,m^{-1}$, which implies $\lambda = 0.1597 \times 3.29 = 0.525$ m. This value allows the computation of a_{max} such as $a_{max} = \lambda + y_0 = 0.525 + 0.65 = 1.175$ m.

Applying the proposed approximate model (see Table 2) $\lambda/\overline{Q} = 1/\sqrt{\eta} \times C \times F_{r0}^{-K} = 1/\sqrt{0.65} \times 0.164 \times 2^{-0.337} = 0.161\ s\,m^{-1}$. It results then $\lambda = 0.161 \times 3.29 = 0.53$ m. Finally $a_{max} = \lambda + y_0 = 0.53 + 0.65 = 1.18$ m.

According to Defina & Susin (2003), the maximum value of the gate opening to restore initial flow conditions is $a_{max} = 1.116$ m. The resulting hysteresis loop is shown in Figure 8.

Table 3 summarizes the comparison between the experimental measurements of Defina & Susin (2003) and the proposed theoretical approach. As can be seen, there is a very good agreement between the theoretical results and the experimental observation with a maximum deviation of around 5%.

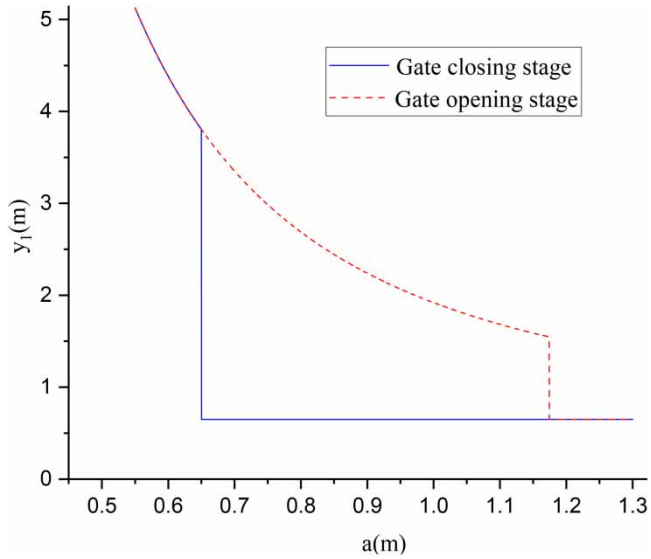

Figure 8 | Hysteresis loop extent in the rectangular channel of Application 1.

Table 3 | Comparison between the theoretical results and experimental data of Defina & Susin (2003)

	Defina & Susin's (2003) experimental measurements	Complete theoretical analysis	Proposed approximate model (Table 2)
a_{max} (m)	1.116	1.175	1.180
Deviation (%)	/	5.29	5.73

7.2. Application 2

Let us consider a parabolic-shaped channel described by the function $y = \kappa x^2$, with $\kappa = 1$. The channel slope and the roughness coefficient are $S = 0.016$ and $n = 0.013$, carrying a flow of 11 $m^3 s^{-1}$. The objective is to determine the maximum gate opening value for the hydraulic jump to disappear from the channel when the gate decreases from 2.5 to 1 m and then returns to 2.5 m.

Using Manning's equation, we obtain the normal flow depth $y_0 = 1.2$ m, implying $F_{r0} = 2.24$.

The resulting top width is then $T = (2/\sqrt{\kappa})\sqrt{y} = 2.19$ m. In the same way as before, the calculation procedure for Application 2 is:

$\eta = y_0/1 = 1.2/1 = 1.2$ and $\overline{Q} = Q/T = 11/2.19 = 5.02\ m^3 s^{-1} m^{-1}$. Using Equation (19), $\overline{\kappa} = 4\eta = 4 \times 1.2 = 4.8$. From Equation (10) $P = 10.48$. By substituting the value of P in Equation (9), one obtains $\omega = 0.468$ which gives $y_0^{conj} = y_0/\omega = 1.2/0.468 = 2.56$ m.

When $a = y_0$ then $F_{r2} = 5.96$ and according to Equation (7), $y_1 = 9.44$ m. In this case, $\lambda/\overline{Q} = 0.198\ s\,m^{-1}$ implying $\lambda = 0.198 \times 5.02 = 0.994$ m leading to the value of $a_{max} = \lambda + y_0 = 0.994 + 1.2 = 2.194 \cong 2.2$ m.

Therefore, the maximum sluice gate opening value so that the hydraulic jump disappears from the upstream channel is $a_{max} = 2.2$ m. The resulting hysteresis loop is depicted in Figure 9.

Applying the proposed explicit approximate model (Table 2) $\lambda/\overline{Q} = 1/\sqrt{\kappa} \times C \times F_{r0}^{-K} = 1/\sqrt{4.8} \times 0.621 \times 2.24^{-0.443} = 0.198\ s\,m^{-1}$, allowing the determination of the value $\lambda = 0.198 \times 5.02 = 0.994$ m. Finally, $a_{max} = \lambda + y_0 = 0.994 + 1.2 = 2.194 \cong 2.2$ m, which is the exact value found above.

7.3. Application 3

In this example, a flow $Q = 5\ m^3 s^{-1}$ is conveyed in a triangular channel with sidewalls making an angle $\theta = 50°$ with the horizontal. Furthermore, the channel slope and the roughness coefficient are $S = 0.02$ and $n = 0.013$, respectively.

If the sluice gate has been lowered from 2.2 to 0.95 m and then raised again to 2.2 m, then it is required to determine the maximum value of the gate opening necessary to restore the initial flow conditions.

The normal depth is $y_0 = 1.06$ m (i.e. $\eta = 1.06/1 = 1.06$) which results in $F_{r0} = 2.33$.

The sidewall parameter $m = 1/\tan(\theta) = 1/\tan(50°) = 0.839$ leading to a top width $T = 2\,m\,y_0 = 2 \times 0.839 \times 1.06 = 1.778$ m. From Equation (20) $\overline{Q} = Q/T = 5/1.778 = 2.812\ m^3 s^{-1} m^{-1}$. Using Equation (18), $\overline{m} = 1/2\eta = (1/2 \times 1.06) = 0.472$. Then, from Equation (10) $P = 15.426$. By reporting the value of P in Equation (9),

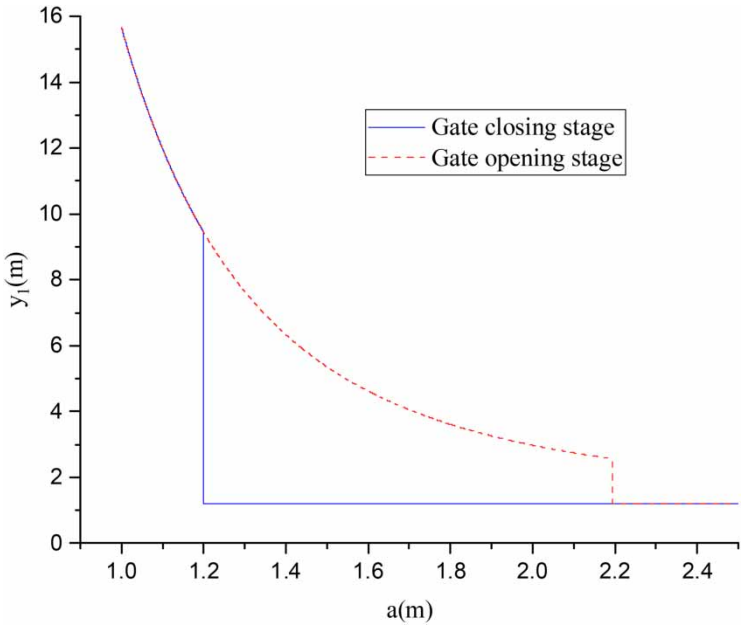

Figure 9 | Hysteresis loop extent in the parabolic channel of Application 2.

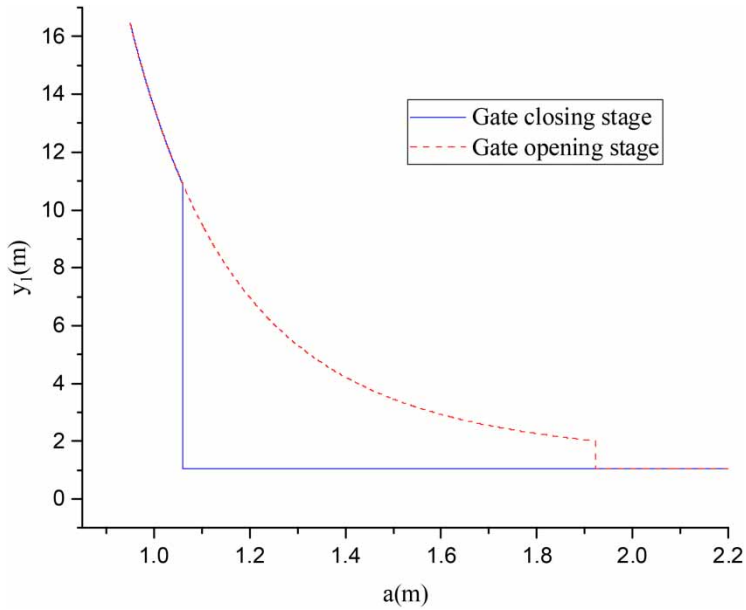

Figure 10 | Hysteresis loop extent in the triangular channel of Application 3.

it results in $\omega = 0.5267$ which gives $y_0^{conj} = y_0/\omega = 1.06/0.527 = 2.01\,\text{m}$. Replacing the value of $F_{r2} = 7.95$ when $a = y_0$ in Equation (7) gives the water depth immediately upstream of the gate $y_1 = 10.87\,\text{m}$ such as $C_c\_\text{new} = C_c\_\text{init}$.

Repeating the process from step 10 for each sluice gate opening, one finds $\lambda/\overline{Q} = 0.306\,\text{s}\,\text{m}^{-1}$, implying $\lambda = 0.306 \times 2.812 = 0.86\,\text{m}$, which results in $a_{max} = \lambda + y_0 = 0.86 + 1.06 = 1.92\,\text{m}$. The maximum sluice gate opening required to restore the initial flow conditions is therefore $a_{max} = 1.92\,\text{m}$. The resulting hysteresis loop is illustrated in Figure 10.

When applying the proposed approximate model (Table 2) $\lambda/\overline{Q} = \sqrt{\overline{m}} \times C \times F_{r0}^{-K} = \sqrt{0.472} \times 0.71 \times 2.33^{-0.535} = 0.31\,\text{s}\,\text{m}^{-1}$. It follows that $\lambda = 0.31 \times 2.812 = 0.872\,\text{m}$, which gives $a_{max} = \lambda + y_0 = 0.872 + 1.06 = 1.932\,\text{m}$.

The deviation of the approximate model from the exact value is then $(|0.306 - 0.31|/0.306) \times 100 = 1.3\%$

The summary of the results of the computation procedure are listed in Table 4.

8. CONCLUSION

This paper presents a theoretical approach for hysteresis loop computation in power-law channels under supercritical flow conditions through a vertical sluice gate. The primary objective was to investigate the hysteretic behavior of the flow considering three channel shapes rectangular, parabolic, and triangular and propose simplified explicit models for hysteresis loop extent computation.

The focus of the study was to understand the hysteretic behavior of flow through a vertical sluice gate, with the specific aim of determining the maximum gate opening required to restore undisturbed flow conditions, thereby eliminating the hydraulic jump from the upstream channel.

By employing energy and momentum equations, expressions for alternate and conjugate depths upstream of the gate were given, leading to second, third, and fourth-degree polynomials for rectangular, parabolic, and triangular channels, respectively.

The extensive computational analysis of hysteresis loops revealed a strong correlation between the maximum gate opening necessary for restoring initial flow conditions and the incident Froude number, as well as the contraction induced by the sluice gate. Additionally, an original approximate solution based on the implicit Von Mises equation for predicting the contraction coefficient was proposed.

Furthermore, the study resulted in the development of explicit simplified models derived from numerical computations of hysteresis loops across a wide range of Froude numbers and dimensionless parameters describing channel geometry. The obtained results show a very satisfactory agreement between the models derived from the suggested approach and the few

Table 4 | Summary of results for the Applications 2 and 3

Parameters	Application 2 (parabolic-shaped channel)	Application 3 (triangular-shaped channel)
y_0	1.2	1.06
F_{r0}	2.24	2.33
T	2.19	1.778
η	1.2	1.06
$\overline{Q}$	5.02	2.812
$\overline{\kappa}$	4.8	/
$\overline{m}$	/	0.472
P	10.48	15.426
ω	0.468	0.526
y_0^{conj}	2.56	2.01
F_{r2}, when $(a = y_0)$	5.96	7.95
y_1	9.44	10.87
$\lambda/\bar{Q}$	0.198	0.306
λ	0.994	0.86
$a_{\max}$	2.2	1.92
Solution using proposed approximate models (Table 2)		
$\lambda/\bar{Q}$	0.198	0.31
λ	0.994	0.872
$a_{\max}$	2.2	1.932

results found in the literature. Unfortunately, a large gap exists in the specialized literature with very rare experimental results regarding the hysteresis phenomenon in power-law channels for a complete validation.

Overall, this research contributes to the understanding of flow behavior in channels with power-law profiles controlled by a sluice gate. Furthermore, this approach offers a valuable tool for predicting the hysteresis phenomenon in the hydraulic engineering of open channels.

DATA AVAILABILITY STATEMENT

All relevant data are included in the paper or its Supplementary Information.

CONFLICT OF INTEREST

The authors declare there is no conflict.

REFERENCES

Abecasis, F. M. & Quintela, A. (1961) Problems of Hydraulic Hysteresis on Steady Free Surface Flow, *Proceedings, 9th General Meeting, International Association for Hydraulic Research*, Dubrovnik, Croatia.

Abecasis, F. M. & Quintela, A. C. (1964) Hysteresis in steady free-surface flow, *Water Power*, **4**, 147–151.

Achour, B. & Khattaoui, M. (2013) Hysteresis of the hydraulic jump controlled by sill in a rectangular channel, *Dam Engineering*, **XXIII** (4), 207–221.

Austria, P. M. (1987) Catastrophe model for the forced hydraulic jump, *Journal of Hydraulic Research*, **25** (3), 269–280.

Baines, P. G. (1984) A unified description of two-layer flow over topography, *Journal of Fluid Mechanics*, **146**, 127–167.

Barenblatt, G. I. (1996) *Scaling, Self-Similarity, and Intermediate Asymptotics: Dimensional Analysis and Intermediate Asymptotics (No. 14)*. Cambridge University Press, New York, USA.

Benjamin, T. B. (1956) On the flow in channels when rigid obstacles are placed in the stream, *Journal of Fluid Mechanics*, **1** (2), 227–248.

Betts, P. L. (1978) Discussion of 'Numerical solution for flow under sluice gates', *Journal of the Hydraulics Division*, **104** (2), 313–315.

Chaudhry, M. H. (2008) *Open-channel Flow*. New York: Springer, p. 523.

Chow, V. T. (1959) *Open-channel Hydraulics*. New York: US Army Corps of Engineers, Hydrologic Engineering.
Cisotti, U. (1908) Vene fluenti, *Rendiconti del Circolo Matematico di Palermo (Flowing Veins. Reports of the Mathematical Circle of Palermo) (1884–1940)*, **25** (1), 145–179.
Daneshfaraz, R., Sadeghfam, S., Aminvash, E. & Abraham, J. P. (2022) Experimental investigation of multiple supercritical flow states and the effect of hysteresis on the relative residual energy in sudden and gradual contractions, *Iranian Journal of Science and Technology, Transactions of Civil Engineering*, **46** (5), 3843–3858.
Defina, A. & Susin, F. M. (2003) Hysteretic behavior of the flow under a vertical sluice gate, *Physics of Fluids*, **15** (9), 2541–2548.
Defina, A. & Susin, F. M. (2006) Multiple states in open channel flow. In: (Brocchini, M. & Trivellato, F, eds). *Vorticity and turbulence effects in fluid structures interactions-advances in fluid mechanics*. Southampton: Wessex Institute of Technology Press. p.105–130.
Defina, A. & Viero, D. P. (2010) Open channel flow through a linear contraction, *Physics of Fluids*, **22** (3), 036602.
Dhar, M., Das, G. & Das, P. K. (2021) Planar hydraulic jump and associated hysteresis in near horizontal confined flow, *Physical Review Fluids*, **6** (8), 084803.
Issacs, L. T. (1977) Numerical solution for flow under sluice gates, *Journal of the Hydraulics Division*, **103** (5), 473–481.
James, C. S. (2020) *Hydraulic Structures*. Berlin: Springer, p 369.
Lawrence, G. A. (1987) Steady flow over an obstacle, *Journal of Hydraulic Engineering*, **113** (8), 981–991.
Marchi, E. (1953) Sui fenomeni di efflusso piano da luci a battente, *Annali di Matematica Pura ed Applicata (The Study of two-Dimensional Flow Through A Submerged Orifice Under A Flat Sluice Gate. Annals of Pure and Applied Mathematics)*, **35** (1), 327–341.
Mehrotra, S. C. (1974) Hysteresis effect in one-and two-fluid systems, in *Proceedings of the Fifth Australasian Conference on Hydraulics and Fluid Mechanics*, edited by D. Lindley and A.J. Sutherland. University of Canterbury, Christchurch, pp. 452–461.
Montes, J. S. (1997) Irrotational flow and real fluid effects under planar sluice gates, *Journal of Hydraulic Engineering*, **123** (3), 219–232.
Muskatirovic, D. & Batinic, D. (1977). The influence of abrupt change of channel geometry on hydraulic regime characteristics, *Proc., 17th Int. Association for Hydraulic Research Congress*, Univ. of Canterbury, Baden-Baden, Germany, 397–404.
Pajer, G. (1937) Über den Strömungsvorgang an einer unterströmten scharfkantigen Planschütze (Over the flow process at a submerged sharp-edged weir), *ZAMM-Journal of Applied Mathematics and Mechanics/Zeitschrift für Angewandte Mathematik und Mechanik*, **17** (5), 259–269.
Pandey, K. K., Subramanya, K. & Kumar, N. (2018) Exact solutions of alternate depth ratio for three exponential channels, *ISH Journal of Hydraulic Engineering*, **26** (3), 310–318. https://www.tandfonline.com/doi/abs/10.1080/09715010.2018.1487805.
Pratt, L. J. (1983) A note on nonlinear flow over obstacles, *Geophysical & Astrophysical Fluid Dynamics*, **24** (1), 63–68.
Quintela, A. C. & Abecasis, F. M. (1979) *Hysteresis in the Transition from Supercritical to Subcritical Flow; Memoria n. 523*. Lisbon: Laboratorio National de Engeharia Civil.
Rajaratnam, N. (1977) Free flow immediately below sluice gates, *Journal of the Hydraulics Division*, **103** (4), 345–351.
Rajaratnam, N. & Subramanya, K. (1967) Flow equation for the sluice gate, *Journal of the Irrigation and Drainage Division*, **93** (3), 167–186.
Rajaratnam, N. & Humphries, J. A. (1982) Free flow upstream of vertical sluice gates, *Journal of Hydraulic Research*, **20** (5), 427–437.
Roth, A. & Hager, W. H. (1999) Underflow of standard sluice gate, *Experiments in Fluids*, **27** (4), 339–350.
Sedov, L. I. (1959) *Similarity and Dimensional Methods in Mechanics*. New-York: Academic Press Inc.
Vanden-Broeck, J. M. (1997) Numerical calculations of the free-surface flow under a sluice gate, *Journal of Fluid Mechanics*, **330**, 339–347.
Vatankhah, A. R. (2017) General solution of conjugate depth ratio (power-law channels), *Journal of Irrigation and Drainage Engineering*, **143** (9), 1–6.
Viero, D. P. & Defina, A. (2017) Extended theory of hydraulic hysteresis in open-channel flow, *Journal of Hydraulic Engineering*, **143** (9), 1–8.
Viero, D. P. & Defina, A. (2019) Multiple states in the flow through a sluice gate, *Journal of Hydraulic Research*, **57** (1), 39–50.
Von Mises, R. (1917) Berechnüng von ausfluss und Überfallzahlen (Discharge and overflow numbers calculation), *Zeitschrift des Vereines Deutscher Ingenieure*, **61** (21), 447–452.
Yen, J. F., Lin, C. H. & Tsai, C. T. (2001) Hydraulic characteristics and discharge control of sluice gates, *Journal of the Chinese Institute of Engineers*, **24** (3), 301–310.
Zwillinger, D. (2018) *CRC Standard Mathematical Tables and Formulas*. Boca Raton, FL: Chapman and Hall/CRC.

First received 25 April 2024; accepted in revised form 25 August 2024. Available online 27 September 2024